

# Whispering Gallery Mode Hemisphere Dielectric Resonators With Impedance Plane

Alexander A. Barannik, Sergey A. Bunyaev, *Student Member, IEEE*, Nickolay T. Cherpak, *Senior Member, IEEE*, Yurii V. Prokopenko, Anna A. Kharchenko, *Student Member, IEEE*, and Svetlana A. Vitusevich

**Abstract**—The electrodynamic characteristics of a high- $Q$  dielectric whispering gallery mode resonator in the form of a hemisphere positioned on an impedance plane were studied. The analysis of the anisotropic resonator was modeled using Maxwell equations and the impedance Leontovich boundary condition. The interaction coefficient  $A_S^j$  of the conductor and microwave field was determined using a frequency and field distribution of the  $j$ -type mode in the hemisphere resonator considering a perfect conducting plane. Results of the theoretical study and experimental measurements of the Teflon resonator frequency spectrum and  $Q$  factor are in good agreement. The results obtained are confirmed by calculations using Microwave Studio CST 2008. In the case of the sapphire hemispherical resonator with an impedance plane, comparison of the experimental and simulation results allows us to identify the  $H$ -type modes in the resonator and their electromagnetic field distribution. In such anisotropic hemisphere resonators, the quasi-TE modes are revealed. The modes are excited together with TE modes inherent to the isotropic resonator and they have an identical distribution of electromagnetic field.

**Index Terms**—Dielectric resonators, electromagnetic fields, frequency, impedance measurement, millimeter-wave measurements,  $Q$  factor.

## I. INTRODUCTION

**Q**UASI-OPTICAL dielectric resonators excited on whispering gallery modes have found applications in a wide frequency range: from microwave [1] to optical [2] bands. Increased interest in such resonators is related to their high  $Q$  factor and higher operation frequencies due to the larger dimensions of the whispering gallery mode resonator

Manuscript received January 29, 2010; revised June 16, 2010; accepted July 09, 2010. Date of publication September 09, 2010; date of current version October 13, 2010. This work was supported by the Federal Ministry of Education and Research, Germany under BMBF Project UKR 08/008.

A. A. Barannik, N. T. Cherpak, Y. V. Prokopenko, and A. A. Kharchenko are with the Institute for Radiophysics and Electronics, National Academy of Sciences of Ukraine, Kharkov 61085, Ukraine (e-mail: a.a.barannik@mail.ru; sergiy.cherpak@ire.kharkov.ua; n.t.cherpak@gmail.com; prokopen@ire.kharkov.ua; ann220286@ya.ru).

S. A. Bunyaev was with the Institute for Radiophysics and Electronics, National Academy of Sciences of Ukraine, Kharkov 61085, Ukraine. He is now with the Departamento de Física da Faculdade de Ciências, IFIMUP and IN—Institute of Nanoscience and Nanotechnology, Universidade do Porto, 4169-007 Porto, Portugal (e-mail: bunyayev@gmail.com).

S. A. Vitusevich is with the Institute of Bio- und Nanosystems (IBN) and the Jülich-Aachen Research Alliance for Future Information Technology (JARA-FIT), 52425 Jülich, Germany (e-mail: s.vitusevich@fz-juelich.de).

Color versions of one or more of the figures in this paper are available online at <http://ieeexplore.ieee.org>.

Digital Object Identifier 10.1109/TMTT.2010.2065870

in comparison to dielectric resonators excited on fundamental modes. They are used in the microwave frequency range for the development of high-quality filters [3] and of oscillators with decreased phase noise and high-frequency stabilization [4]–[6], and also for the power combining of several oscillators [7].

They also can be used for the measurement of the complex permittivity of dielectric substances [8], [9], surface impedance of high-temperature superconducting (HTS) films [10]–[12], and studies of semiconductor properties [13], [14].

The increasing sensitivity in the microwave band is important for HTS surface impedance measurements, the development of HTS-based devices, and for a deeper understanding of the nature of unconventional superconductivity phenomena. Obtaining surface impedance data for HTS material is of great significance in a broad temperature range including very low temperatures where the highest sensitivity of microwave loss measurement is required [15].

Resonators excited on whispering gallery modes are usually studied and used in the form of circular cylinders (see, e.g., [16]–[18]). It should be noted that [18] was one of the first papers that compared the matching of theory and experiment in the case of anisotropic dielectric resonators. Recently, it has been shown that these resonators with conducting endplates can be used for measurement of HTS thin-film surface resistance [10], [11], [19]. Such an approach allows enhancing the accuracy of small surface resistance  $R_S$ , value measurement due to the increased  $Q$  factor of the resonator, and means there is no need for a calibration procedure of measurement setup. In addition, the possibility of measuring the films with different forms and dimensions is an additional advantage. However, the measured  $R_S$  is the averaged value of two films. In principle, individual  $R_S$  values of conducting endplates can be found by using a so-called “round robin” procedure [20], which requires three thermal cycle measurements of three different pairs of HTS films and is a very time-consuming procedure.

Therefore, resonators have recently been developed in a form that allows only one conducting endplate to be studied. In such a resonator, the microwave field has to be localized near the conducting surface. The resonator can be designed in the form of a truncated cone [21] or a hemisphere [22] placed on a conducting plane, i.e., a conducting endplate. It was shown experimentally that, in these resonators, whispering gallery modes can be excited near the surface of the plate, i.e., close to the resonator base [23]. The resonator in the form of a truncated cone was studied in [24]. However, the electrodynamic of hemispherical resonators has not been explored in detail, which substantially hinders their application.

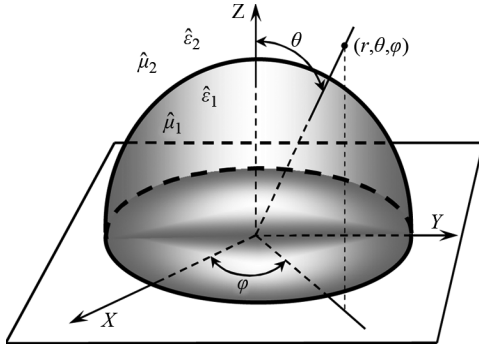


Fig. 1. Hemispherical dielectric resonator with conducting infinite plane.

In this paper, we report on the results of a theoretical and experimental study of hemispherical whispering gallery mode resonators with an impedance plane. Microwave properties of the resonators designed on the basis of isotropic and anisotropic dielectrics were analyzed. The experiment and theory were found to be in good agreement.

## II. THEORY

Hemispherical resonators are very promising for practical applications in a microwave technique. It is evident that the electrodynamics of a spherical whispering gallery modes resonator is a starting point for theoretical studies of a hemispherical resonator with a plane conducting surface. Recently, the authors of [25] and [26] theoretically analyzed the whispering gallery mode resonator in the form of a sphere made of anisotropic dielectric, taking into account that most materials with a small loss are anisotropic. At the same time, analyzing the effect of dielectric anisotropy on the electromagnetic properties of hemispherical whispering gallery mode resonators remains the most important issue of the day. The dependence of hemispherical whispering gallery mode resonator eigenfrequencies and  $Q$  factor on impedance properties of the plane surface have to be studied.

### A. Hemispherical Dielectric Resonator With Perfect Conducting Plate

Electromagnetic fields of the eigen  $p$ -mode of a hemispherical dielectric resonator with a perfect conducting plane surface (Fig. 1) can be calculated using Maxwell equations

$$\begin{aligned} \text{rot} \vec{H}_{p\nu} &= \frac{1}{c} \frac{\partial}{\partial t} (\hat{\epsilon}_\nu \vec{E}_{p\nu}) \\ \text{rot} \vec{E}_{p\nu} &= -\frac{1}{c} \frac{\partial}{\partial t} (\hat{\mu}_\nu \vec{H}_{p\nu}) \end{aligned} \quad (1)$$

where material equations were taken into account.

Here,  $\vec{E}_{p\nu}$  and  $\vec{H}_{p\nu} \sim \exp(-i\omega_p t)$ , where  $t$  is the time and  $\omega_p$  is the eigen complex frequency of the resonator with a  $p$ -mode:  $\omega_p = \omega'_p - i\omega''_p$ ,  $\omega''_p \geq 0$ ;  $\hat{\epsilon}_\nu$  and  $\hat{\mu}_\nu$  are the tensors of permittivity and permeability of the  $\nu$ -medium, counting from the center of the studied resonator taking into account the surrounding environment;  $c$  is the velocity of light. Tensor components  $\hat{\epsilon}_\nu$  and  $\hat{\mu}_\nu$  are complex values and characterize the anisotropic properties of  $\nu$ -medium with loss. If the media of the resonator or surrounding environment are isotropic with respect

to electric or magnetic fields, they are characterized by corresponding tensors  $\hat{\epsilon}_\nu$  or  $\hat{\mu}_\nu$ , matrices of which have a diagonal form with the same components. Using such an approach, all expressions obtained by analysis of the case of anisotropic resonator can be transformed easy into those suitable for analysis of the isotropic resonator case. Index  $p$  consists of three mode indices, namely,  $n m s$ . Azimuthal mode index  $m$  has magnitudes  $m = 0, 1, 2, 3, \dots$ , and equals half a number of field variations along angle  $\varphi$ . At the same time, index  $m \leq n$ , where a polar index  $n$  is determined through the quantity of field variations  $\bar{p}$  along the polar angle  $\theta$  in a spherical coordinate system:  $n = 2\bar{p} + m - 1$ . We used the relation between indices  $n$  and  $m$  and quantity of field variations ( $p$  with bar accent) along the polar angle taking into account the field distribution on a sphere surface of the resonator [27], which is generally determined by the associated Legendre function. The radial index  $s$ , which is an ordinal number of the root of the characteristic equation for the studied resonator, corresponds to the quantity of field variations along a radial coordinate  $r$ . Expressions for electric and magnetic vector components of the  $j$ -type  $p$ -mode are used as in [25] and [27]. In the case of isotropic media in the resonator and surrounding environment, the eigencomplex frequencies  $\omega_p$  are determined by solving a corresponding characteristic equation [27]. For the  $j$ -type mode, we assume  $E$  or  $H$ , i.e., eigen TM or TE modes, respectively (and additional quasi-TM or quasi-TE modes for the anisotropic resonator or in the presence of an anisotropic environment). We have found experimentally that additional quasi-TE modes appear in the case of an anisotropic hemisphere. These modes are absent in isotropic resonators. In hemispherical dielectric resonators, a sum of indices  $n + m$  has odd numbers for eigen  $E$ -type modes and even numbers for  $H$ -type modes [27].

One-mode approach used in solving the electrodynamic problem is justified by the physical background. In the experimental studies, the resonator is excited by some source positioned in the definite point of the space. The source forms monochromatic radiation. As a result of frequency and space selection, as a rule, only one mode is excited in the resonator. A spatial selection is provided by positioning the excitation source in the field maximum of the resonator eigenmode. Therefore, a superposition field of excited modes with the same frequency is formed mainly by the field of the dominant eigenmode in the resonator. This fact exhibits in a theory of stimulated oscillations in the resonator under study, when we solve the electrodynamic problem using a separation of variables. At the same time, we obtain components of the field formed by a superposition of the fields of eigenmodes with the same frequency. The main contribution to the field is introduced by a dominant mode, determined by a spatial selection implemented using the excitation source. Therefore, in a theory of eigenmodes, it is sufficient to study the influence of imperfect conductivity of a plane surface on the field of one (dominant) mode. In addition, in a case of an isotropic resonator with a perfect conducting plane, electrodynamic analysis reduces to a solution of independent differential equations for degenerate TM and TE modes with the same polar indices. The effect of the conducting plane results in the resonator spectrum sparseness, determined by boundary conditions on

the conducting surface, and manifested itself in a sum of polar and azimuthal indices. The field distribution pattern of these modes indicates the possibility of their selection using a polar coordinate [27]. Thus, the vector fields with mode indices  $p$  in (1) describe the resulting electric and magnetic fields whose structure corresponds to the dominant mode in a resonator with a perfectly conducting plane surface.

The energy of the electromagnetic field created by the  $p$ -mode of  $j$ -type in the resonator with a perfect conducting plane is determined by the expression [28]

$$W_p^j = \frac{1}{8\pi} \sum_{\nu} \int_{V_{\nu}} \left( \vec{H}_{p\nu} \hat{\mu}'_{\nu} \vec{H}_{p\nu}^* + \vec{E}_{p\nu} \hat{\epsilon}'_{\nu} \vec{E}_{p\nu}^* \right) dV. \quad (2)$$

where integration is performed over a total volume  $V_{\nu}$  of medium  $\nu$ , and tensor components  $\hat{\epsilon}'_{\nu}$  and  $\hat{\mu}'_{\nu}$  are real magnitudes that characterize the anisotropic properties of the  $\nu$ -medium without losses. Here, electric  $\vec{E}_{p\nu}$  and magnetic  $\vec{H}_{p\nu}$  fields are represented by resolutions of vectors of identical fields (the  $p$ -mode of  $j$ -type) in a resonator in a spherical coordinate system  $\vec{E}_{p\nu} = E_{r p\nu} \vec{e}_r + E_{\theta p\nu} \vec{e}_{\theta} + E_{\varphi p\nu} \vec{e}_{\varphi}$  and  $\vec{H}_{p\nu} = H_{r p\nu} \vec{e}_r + H_{\theta p\nu} \vec{e}_{\theta} + H_{\varphi p\nu} \vec{e}_{\varphi}$ , where  $\vec{e}_r$ ,  $\vec{e}_{\theta}$ , and  $\vec{e}_{\varphi}$  are unit vectors of the corresponding axes. The elementary volume  $dV$  and limits of integration in accordance with the geometry of the resonator are also taken in the spherical coordinate system. Here and below, the symbol “\*” indicates complex conjugation.

### B. Resonator With Impedance Plane

Imperfect conductivity of a plane surface has a considerable influence on the spectral and energy characteristics of the resonators (Fig. 1) [29], [30]. They are determined by solutions of the set of homogeneous equations

$$\begin{aligned} \text{rot} \vec{H}_{\nu} &= \frac{1}{c} \frac{\partial}{\partial t} \left( \hat{\epsilon}_{\nu} \vec{E}_{\nu} \right) \\ \text{rot} \vec{E}_{\nu} &= -\frac{1}{c} \frac{\partial}{\partial t} \left( \hat{\mu}_{\nu} \vec{H}_{\nu} \right) \end{aligned} \quad (3)$$

where  $\vec{E}_{\nu}$  and  $\vec{H}_{\nu} \sim \exp(-i\omega t)$ , and  $\omega = \omega' - i\omega''$  is the eigenfrequency of the resonator ( $\omega'' \geq 0$ ). It should be noted that both (1) and (3) have to be written for the correct mapping technique for obtaining integral (5).

In the opposite case to the perfect conductor, the electromagnetic field in a real conductor penetrates into the depth of the skin layer, the thickness of which is finite and small, especially in the microwave frequency range. In this respect, the perfect conductor in the main reflects the real metal conductor properties [31]. However, Joule heat losses are equal to zero in a perfect conductor, and if it is necessary to take them into account, the idea of a perfect conductor cannot be applied. These losses exist in a real conductor, and their value increases with decreasing skin layer. The case of a real conductor can be considered in an electrodynamic study by taking into account the impedance boundary condition (Leontovich boundary condition) on its surface [31]

$$\left[ \vec{n}_0, \vec{E}_{\nu} \right] = -\frac{c}{4\pi} Z_S \left[ \vec{n}_0, \vec{H}_{\nu} \right] \quad (4)$$

where  $\vec{n}_0$  is the normal vector directed into the conductor toward the surface,  $Z_S = R_S - iX_S$  is the surface impedance with  $R_S$  and  $X_S$ —the surface resistance and surface reactance of a conductor, respectively. Fields  $\vec{E}_{\nu}$  and  $\vec{H}_{\nu}$  in (4) correspond to their values in the points of the  $\nu$ -medium, which are infinitely near, but do not belong to a conductor surface. The relation (4) is an approximation and is feasible in the case of a strong skin effect, when: 1) a field penetration depth in a conductor is much smaller than a wavelength in the  $\nu$ -medium and 2) a skin layer thickness is small in comparison to the conductor thickness and radius of curvature of the surface. It should be emphasized that, in (4), both penetration of the electromagnetic field into the conductor and corresponding losses are taken into account. According to [31], the fractional error is related to the influence of the conductor on the electromagnetic field and is of the order of magnitude  $1/|\epsilon_{\nu}\mu_{\nu}|$ , where permittivity  $\epsilon_{\nu}$  and permeability  $\mu_{\nu}$  correspond to the conductor medium.

After multiplying the set of complex conjugate (3) by  $(-\vec{E}_{\nu})$ ,  $\vec{H}_{\nu}$ , respectively, and the set (1) by complex conjugate magnitudes  $(-\vec{E}_{p\nu}^*)$ ,  $\vec{H}_{p\nu}^*$ , we add them. After integrating the obtained expression over the total space taking into account, the divergence theorem and using the continuity conditions of tangential-field components on the spherical surface of the resonator ( $r = r_1$ ) and also the impedance boundary condition (4) on the plane  $z = 0$  ( $\theta = \pi/2$ ), we obtain the integral equation in the form

$$\begin{aligned} (\omega - \omega_p^*) \sum_{\nu} \int_{V_{\nu}} \left( \vec{H}_{\nu} \hat{\mu}'_{\nu} \vec{H}_{p\nu}^* + \vec{E}_{\nu} \hat{\epsilon}'_{\nu} \vec{E}_{p\nu}^* \right) dV \\ + i(\omega + \omega_p^*) \sum_{\nu} \int_{V_{\nu}} \left( \vec{H}_{\nu} \hat{\mu}''_{\nu} \vec{H}_{p\nu}^* + \vec{E}_{\nu} \hat{\epsilon}''_{\nu} \vec{E}_{p\nu}^* \right) dV \\ = i \frac{c^2}{4\pi} Z_S \sum_{\nu} \int_{S_{\nu}} \left[ \vec{e}_z \left[ \vec{e}_z, \vec{H}_{\nu} \right] \right] \vec{H}_{p\nu}^* dS. \end{aligned} \quad (5)$$

The integration on the left is performed over the total volume  $V_{\nu}$  of the  $\nu$ -medium and on the right over the conducting plane surface  $S_{\nu}$  contacting with the  $\nu$ -medium. It should be noted that fields  $\vec{H}_{\nu}$  and  $\vec{H}_{p\nu}$ , included in (5) on the right, correspond to field magnitudes in the  $\nu$ -medium points infinitely near to the conductor surface. The vector  $\vec{e}_z = -\vec{n}_0$  is the unit vector of the  $Z$ -axis.

The fields  $\vec{E}_{\nu}$  and  $\vec{H}_{\nu}$  are represented in the eigenmode subsetting of  $\vec{E}_{p\nu}$  and  $\vec{H}_{p\nu}$  for a resonator with a perfect conducting surface

$$\begin{aligned} \vec{E}_{\nu} &= \sum_{p'} \beta_{p'} \vec{E}_{p'} \\ \vec{H}_{\nu} &= \sum_{p'} \beta_{p'} \vec{H}_{p'} \end{aligned} \quad (6)$$

where  $\beta_{p'}$  is the subsetting coefficient.

<sup>1</sup>It should be noted that, in electrodynamics, as a rule, quasi-monochromatic fields are used with time dependence in the form of  $\exp(-i\omega t)$ , which gives a sign “minus” in the expression for surface impedance  $Z_s$  (see, e.g., [32]). In contrast, in microwave superconductivity, the time dependence is used in the form of  $\exp(i\omega t)$ , which changes the sign before the imaginary part of  $Z_s$  (see, e.g., [15] and [33]).

By substituting (6) in (5) and taking into account (2), we obtain the infinite in respect of the  $p$ -modes set of equations

$$[(\omega - \omega_p^*) W_p^j + i(\omega + \omega_p^*) W_{emp}^j] \beta_p = -iZ_S \frac{1}{2} \sum_{p'} I_{p'p}^2 \beta_{p'} \quad (7)$$

where the factor  $W_{emp}^j = 1/8\pi \sum_{\nu} \int_{V_{\nu}} (\vec{H}_{p\nu} \hat{\rho}_{\nu}'' \vec{H}_{p\nu}^* + \vec{E}_{p\nu} \hat{\epsilon}_{\nu}'' \vec{E}_{p\nu}^*) dV$  reflects the energy loss of the electromagnetic field created by the  $p$ -mode of the  $j$ -type in the general case of the anisotropic medium in the resonator studied with a perfect conducting plane.

The parameter of  $I_{p'p}^2 Z_S = -c^2/4g\pi^2 Z_S \sum_{\nu} \int_{S_{\nu}} [\vec{e}_z [\vec{e}_z, \vec{H}_{p'\nu}]] \vec{H}_{p'\nu}^* dS$  includes loss in the surface of the plane with finite conductivity and interaction of the modes in the resonator.

The condition for the existence of nontrivial solutions of the system (7) in regard to  $\beta_{p'}$  can be found from the equation when the determinant is equal to zero

$$\det \left\| \begin{array}{c} [(\omega - \omega_p^*) W_p^j + i(\omega + \omega_p^*) W_{emp}^j] \delta_{p'p} \\ +iI_{p'p}^2 Z_S/2 \end{array} \right\| = 0 \quad (8)$$

where  $\delta_{p'p}$  is the Kronecker symbol. Expression (8) is the equation for determining the eigenfrequencies  $\omega$  of the resonator shown in Fig. 1 with finite conducting plates. Equation (8) physically represents the energy conversation law for quasi-monochromatic fields of resonator eigenmodes. In addition, (8) determines the eigenfrequency shift of the resonator studied with a finite conducting plane in respect of the resonator with a perfect conducting plane.

By neglecting the interaction of modes ( $I_{p'p}^2 = 0$  at  $p' \neq p$ , reflecting that surface current in a conducting plane is induced by a dominant mode field in the resonator), (8) can be reduced to the form

$$\omega - \omega_p^* + i(\omega + \omega_p^*) \frac{W_{emp}^j}{W_p^j} + \frac{i}{2} \frac{I_{pp}^2 Z_S}{W_p^j} = 0 \quad (9)$$

where  $I_{pp}^2 = c^2/4g\pi^2 \sum_{\nu} \int_{S_{\nu}} [(-\vec{e}_z, \vec{H}_{p\nu})]^2 dS$  is the squared surface current in a resonator conducting plane. This current is the result of the penetration of an eigen  $p$ -mode electromagnetic field into the conductor. For the resonator studied  $\vec{e}_z = \vec{e}_{\theta}$  and  $\vec{H}_{p\nu} = H_{rp\nu}|_{\theta=\pi/2} \vec{e}_{\rho} + H_{\theta p\nu}|_{\theta=\pi/2} \vec{e}_{\theta} + H_{\varphi p\nu}|_{\theta=\pi/2} \vec{e}_{\varphi}$ . In the general case, (9) also has to be applied for a resonator with a perfect conducting surface (i.e., at  $Z_S = 0$ ). In such a resonator, the frequencies do not shift and  $\omega = \omega_p$ . Therefore, between the electromagnetic energy  $W_p^j$  and its loss  $W_{emp}^j$  in the resonator (Fig. 1) with a perfect conducting plane, the following relation is fulfilled:  $W_p^j/W_{emp}^j = \omega'_p/\omega''_p$ , which results in a doubling of the value of the eigen  $Q^j$  factor of the resonator with a  $j$ -type mode. Using (9) and  $Z_S = R_S - iX_S$ , the resonator eigenfrequency shift as a result of the finite conductivity of the conducting plane can be described as

$$\omega - \omega_p^* = -\frac{(X_S + iR_S) I_{pp}^2}{2W_p^j} - \frac{i(\omega + \omega_p^*) \omega''_p}{\omega'_p}$$

The shift of the eigenfrequency of the real part of the resonator is determined, in the main, by the imaginary part of surface impedance (by reactance)  $X_S$ . Nondissipative energy stored in the surface layers of the plane wall of the resonator depends on the magnitude of the reactance. Surface resistance  $R_S$  determines the power of the Joule losses  $P_c^j = I_{pp}^2 R_S/2$  in the impedance surface of the studied resonator averaged over the period. Finite conductivity of the surface results in decreasing real parts and increasing imaginary parts of the eigenfrequencies in respect of a resonator with a perfect conducting plane. The effect is caused by the penetration of eigenmode fields into the resonator' conducting plane, which, in turn, is accompanied by an increase in resonator volume. Assuming identical eigenmode field configurations for two resonators with different conductivity of the plane surface, the resonator with the larger surface resistance  $R_S$  and surface reactance  $X_S$  has a smaller value of  $\omega'$ .

In principle, (9) allows us to determine the surface impedance  $Z_S$  of the resonator conducting plane using eigencomplex frequency measured experimentally.

### C. Interaction Between Microwave Field and Resonator Conducting Plane: Conductor Inclusion Factor

In the case of small attenuation of the eigenmode field, i.e., when the decrease in mode amplitude is small and the field can be considered as harmonic within one period, a resonator  $Q$  factor is determined by a ratio of energy  $W_p^j$ , stored in the resonator volume, to the energy  $\Delta W_p^j$ , which is lost per period  $Q_0^j = 2\pi W_p^j/\Delta W_p^j$ . If the mode amplitude in the resonator is kept constant using an external source, compensating the energy losses, the  $Q$  factor can be calculated by

$$Q_0^j = \frac{\omega' W_p^j}{\sum_{\nu} P_{l\nu}^j} \quad (10)$$

where  $\sum_{\nu} P_{l\nu}^j$  is the loss power, which consists of losses in the medium, filling a restricted volume, radiated losses into the surrounding environment, and losses due to the conducting medium  $P_c^j = I_{pp}^2 R_S/2$ . Therefore, the total losses of electromagnetic energy in a resonator with the  $j$ -type mode are determined by the relation

$$\frac{1}{Q_0^j} = \frac{1}{Q^j} + \frac{1}{Q_c^j} \quad (11)$$

Here,  $Q^j$  is the resonator  $Q$  factor determined by radiation loss and loss in the dielectric, and  $Q_c^j$  is determined by the loss in the conducting surface of the resonator. In the case of strong damping of the mode, (10) cannot be applied to find the  $Q$  factor including all loss components, and the following expression should be used  $Q_0^j = \omega'/2\omega''$ , which is correct under any damping of eigenmode in the resonator.

The  $Q$  factor related to both energy loss in the dielectric and radiation can be determined using  $Q^j = \omega'_p/2\omega''_p$ . In the case of exciting weakly damped whispering gallery modes, accordingly to (10), the resonator  $Q$  factor due to loss in the conducting surface is determined by the expression  $Q_c^j = \omega' W_p^j/P_c^j$ . The resonator  $Q_c^j$  factor can be presented in the form of  $Q_c^j = \omega'/\omega'_p A_S^j R_S$ , taking into account  $P_c^j = I_{pp}^2 R_S/2$ . Here,

TABLE I  
CHARACTERISTICS OF THE RESONATOR WITH  $TM_{35\ m\ 1}$  MODES

$m$	$\omega' / 2\pi$ (GHz)		$Q_0^E$		$A_S^E$ (Ohm <sup>-1</sup> )
	copper	brass	copper	brass	
0	35.0796	35.0796	4291.4	4291.4	$6.4342 \times 10^{-9}$
10	35.0796	35.0795	4279.9	4258.6	$1.2845 \times 10^{-5}$
20	35.0795	35.0794	4245.6	4163.0	$5.1355 \times 10^{-5}$
32	35.0794	35.0791	4130.4	3861.3	$1.8542 \times 10^{-4}$
34	35.0794	35.0790	4107.0	3803.4	$2.1357 \times 10^{-4}$

TABLE II  
CHARACTERISTICS OF THE RESONATOR WITH  $TE_{35\ m\ 1}$  MODES

$m$	$\omega' / 2\pi$ (GHz)		$Q_0^H$		$A_S^H$ (Ohm <sup>-1</sup> )
	copper	brass	copper	brass	
1	34.5380	34.5380	4712.8	4712.6	$1.1209 \times 10^{-7}$
11	34.5380	34.5380	4705.4	4691.6	$6.8853 \times 10^{-6}$
21	34.5380	34.5379	4667.3	4584.9	$4.2309 \times 10^{-5}$
31	34.5380	34.5378	4623.0	4464.9	$8.4198 \times 10^{-5}$
33	34.5377	34.5370	4285.9	3668.7	$4.3138 \times 10^{-4}$

the conductor inclusion factor  $A_S^j$  describes the interaction of the microwave field and conducting plane. It depends on the field distribution of the  $j$ -mode near the resonator conducting surface and can be calculated using

$$A_S^j = \frac{I_{pp}^2}{\omega_p' W_p^j}. \quad (12)$$

Hence, the coefficient  $A_S^j$  is determined by the eigenmode frequency and field distribution in a resonator with a perfect conducting plane. In other words,  $A_S^j$  depends on the geometric parameters of a resonator and the electrophysical properties of its media including the surrounding environment and is independent of the properties of the conducting plane. The coefficient  $A_S^j$  is calculated using (12) in the frame of the theory of eigenmodes of the resonator because the squared surface current  $I_{pp}^2$  in the resonator conducting surface and energy  $W_p^j$  of the  $j$ -type eigen  $p$ -mode are determined by field components, which are represented by expressions [25], [27] containing the same constant. It should be noted that, for the resonator under study with a spherical interface of media, the energy  $W_p^j$  can be obtained using an analytical solution. However, the integral relationship  $I_{pp}^2$  can be found only using numerical methods. In the case when the energy  $W_p^j$  includes only the energy of the magnetic field, the inverse value of the conductor inclusion factor  $(A_S^j)^{-1}$  is the geometric factor [34].

Tables I and II summarize the results of numerically studying the hemispherical Teflon resonator of radius  $r_1 = 3.9$  cm with  $TM_{35\ m\ 1}$  and  $TE_{35\ m\ 1}$  modes. The hemisphere is placed on the copper ( $R_S = 49$  m $\Omega$ ) or brass ( $R_S = 140$  m $\Omega$ ) planes.

A resonator with an  $H$ -type mode has the largest values of the coefficient  $A_S^j$  when  $m = n$  and with an  $E$ -type mode when  $m = n - 1$ . This indicates the localization of eigen  $TM_{n\ n-1\ s}$  and  $TE_{n\ n\ s}$  mode electromagnetic fields near the conducting plane of the resonator. This case is important for increasing the sensitivity of the method for impedance determination.

#### D. Eigenfrequencies and $Q$ Factor of Resonator With Impedance Plane

Using the solutions of (9), the solutions of the characteristic equation  $\omega_p$  for the resonator with a perfect conducting plane

[27], the relation  $W_p^j/W_{emp}^j = \omega_p'/\omega_p''$ , and taking into account the conductor inclusion factor  $A_S^j$  from (12), the eigencomplex frequencies  $\omega$  of the resonator (Fig. 1) can be determined by the expression

$$\omega = \omega_p \left( 1 - i \frac{\omega_p'^2 A_S^j Z_S}{2|\omega_p|^2} \right). \quad (13)$$

Since  $Z_S = R_S - iX_S$  and using (13), the real part of the eigenfrequency of a resonator with the  $p$ -mode of  $j$ -type can be reduced to

$$\omega' = \omega_p' \left[ 1 - \frac{1}{2} \frac{\omega_p'^2}{|\omega_p|^2} A_S^j \left( X_S + \frac{\omega_p''}{\omega_p'} R_S \right) \right]. \quad (14)$$

Frequency  $\omega'$  agrees with the resonance frequency measured experimentally in the exciting  $p$ -mode of  $j$ -type in the resonator under conditions of weak coupling between the resonator and exciter. The imaginary part of the eigenfrequency can be determined as

$$\omega'' = \omega' \frac{\omega_p''}{\omega_p'} + \frac{1}{2} \omega_p' A_S^j R_S. \quad (15)$$

Equation (15) corresponds physically to the case when energy total losses  $1/Q_0^j = 2\omega''/\omega'$  in the resonator satisfy (11). This indicates that, in the case of a strong skin effect, the  $Q$  factor of the resonator determined by loss in its conducting surface can be represented in the form of  $Q_c^j = \omega'/\omega_p' A_S^j R_S$ .

In real conductors with a strong skin effect, the surface resistance equals the surface reactance ( $R_S = X_S$ ) and has a positive magnitude that indicates the inductive nature of the surface impedance of the conducting surface of the resonator. This can be explained by the fact that the total surface current  $I_{pp}$  has a phase shift in comparison with the tangential electric field  $[\vec{n}_0, \vec{E}_\nu] = -[\vec{e}_z, \vec{E}_\nu]$  on the conducting surface of the resonator. According to [31], only volume currents on the conducting surface are in phase with the surface electric field, and currents in the deeper layers of conductor have a phase shift from the surface electric field because of wave excitement and propagation along the direction normal to the conductor plane. In a resonator with a real conducting (i.e., impedance) plane surface, the frequency of the eigenmode can be determined using (13) by the expression

$$\omega = \omega_p \left( 1 - \frac{\omega_p'^2 A_S^j R_S (1 + i)}{2|\omega_p'|^2} \right). \quad (16)$$

Therefore, from (16), the real part of the eigenfrequency of a resonator with the  $p$ -mode of  $j$ -type is equal to  $\omega' = \omega_p' [1 - \omega_p'^2 A_S^j R_S (1 + \omega_p''/\omega_p') / 2|\omega_p|^2]$ , which corresponds to the frequency determined by (14) at  $X_S = R_S$ . At the same time, the imaginary part of the frequency is determined by (15), which indicates the universality of (11) for calculating the total energy losses in the resonator. Besides, the real and imaginary parts of the resonator eigenfrequency are related

$$\omega' \left( 1 - \frac{\omega_p''}{\omega_p'} \right) + \omega'' \left( 1 + \frac{\omega_p''}{\omega_p'} \right) = \omega_p' \left( 1 + \frac{\omega_p''^2}{\omega_p'^2} \right). \quad (17)$$

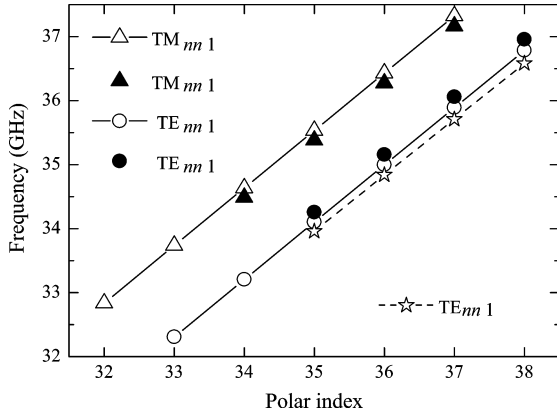


Fig. 2. Eigenfrequencies of the hemispherical resonator designed from Teflon with  $TE_{n n 1}$  and  $TM_{n n 1}$  modes: closed symbols—experimental data, open symbols—calculation results, dashed line represents simulation results using MWS.

Thus, in the general case, the eigenfrequency of the resonator (Fig. 1) with a  $p$ -mode of  $j$ -type is determined by (13). At the same time, the resonator eigen  $Q$  factor is  $Q_0^j = \omega' / 2\omega''$ . When the conducting plane of the resonator is a real metal conductor, the eigenfrequencies of the resonator can be determined by (16).

In the case of an isotropic dielectric hemisphere with a perfect conducting plane surface, the eigen  $E$ -type and  $H$ -type modes are frequency degenerated,  $n$ - and  $(n + 1)$ -fold, respectively [27]. The finite conductivity of the plane surface of the hemisphere dielectric resonator according to (13) removes the frequency degeneration because the factor  $A_S^j$  of (12) is expressed by the ratio of integral relationships for  $I_{pp}^2$  and  $W_p^j$ , which contain the field components for the  $p$ -mode of  $j$ -type depending on the mode indices  $n$ ,  $m$ , and  $s$ .

### III. EXPERIMENTAL STUDY OF HEMISPHERICAL RESONATORS

#### A. Teflon Hemisphere

Teflon is an isotropic material with permittivity measured using a cylindrical disc whispering gallery mode resonator in the present work and determined as  $\epsilon_1 = 2.04(1 + 1.7 \times 10^{-4}i)$ . It demonstrates relatively small losses of eigenmode energy in a resonator made of this material. Moreover, Teflon can be easily machined, which is convenient for producing resonators of different forms. Therefore, we started resonator studies using a hemispherical resonator made of Teflon. The radius of the resonator is  $r_1 = 3.9$  cm. The metal plane of the resonator (Fig. 1) was produced from brass ( $R_S = 140$  m $\Omega$ ). The experimental data on the eigenfrequency and  $Q$  factor were measured using Agilent Network Analyzer PNA-L N5230A in the frequency band from 30 to 40 GHz.

The eigenfrequencies of the resonator with  $TE_{n n 1}$  and  $TM_{n n 1}$  modes at different azimuthal indices  $m = n$  are calculated using the equation  $\omega' = \omega_p' [1 - \omega_p'^2 A_S^j R_S (1 + \omega_p'' / \omega_p')] / 2[\omega_p']^2$ , which was obtained from (14) at  $X_S = R_S$ . The results are compared with the measured values, as well as with those calculated using CST Microwave Studio 2008 (MWS) for the same modes (Fig. 2).

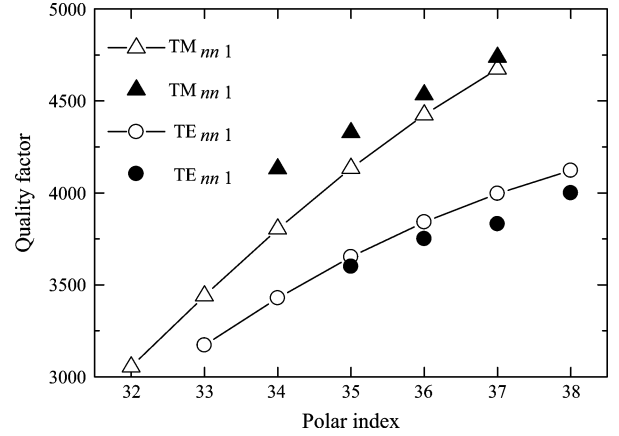


Fig. 3.  $Q$  factor of hemispherical resonator from Teflon with  $TE_{n n 1}$  and  $TM_{n n 1}$  modes: closed symbols—experimental data, open symbols—calculation results.

Fig. 2 demonstrates that the results of the calculated and experimental data are in good agreement for both  $TE_{n n 1}$  ( $H$ -type, for which  $E_{rpn} \equiv 0$ ) and for  $TM_{n n 1}$  ( $E$ -type, for which  $H_{rpn} \equiv 0$ ) modes. This fact confirms that the analytical approach is correct and can be used for spectrum identification of an isotropic hemisphere whispering gallery mode resonator. The experimental and calculated data deviate insignificantly, which is caused by the slight surface roughness of the spherical resonator made from Teflon and the brass plane. The roughness is difficult to take into account in the calculations. For correct identification of the resonator modes excited in the experiment, we compared the field distributions obtained by different methods: 1) calculated using a computer program developed at the Institute of Radiophysics and Electronics, National Academy of Sciences (NAS) of Ukraine; 2) calculated using the program package CST MWS 2008 (transient solver); and 3) measured experimentally using the small perturbation method, i.e., using a small-size test probe. A combination of methods allows us to determine the indices of the modes excited in the resonator.

In addition, the energetic characteristics of the resonator were studied.  $Q$ -factor values of the Teflon resonator with  $TE_{n n 1}$  and  $TM_{n n 1}$  modes are shown in Fig. 3. The calculated  $Q$ -factor values were obtained using (11) taking into account that  $Q^j = \omega_p' / 2\omega_p''$  and  $Q_c^j = \omega' / \omega_p' A_S^j R_S$ . Fig. 3 shows that whispering gallery mode resonator with  $TE_{n n 1}$  and  $TM_{n n 1}$  modes had different values of  $Q$  factor. They increase with increasing azimuthal index  $m = n$ , which, in turn, is accompanied by an increase of the eigenfrequencies. The  $Q$  factors strongly depend on values  $R_S$  and  $\epsilon_1$ . Nevertheless, the difference between the calculated and experimental energetic characteristics for both mode types does not exceed the relative error of the resonator  $Q$ -factor measurement, which corresponds to the value  $\Delta Q_0^j / Q_0^j \approx \pm 5\%$ .

#### B. Sapphire Hemisphere Resonator

In order to study the special electrodynamic features of a hemispheric resonator made of uniaxial anisotropic single crystals, the spectral and energetic characteristics of a sapphire

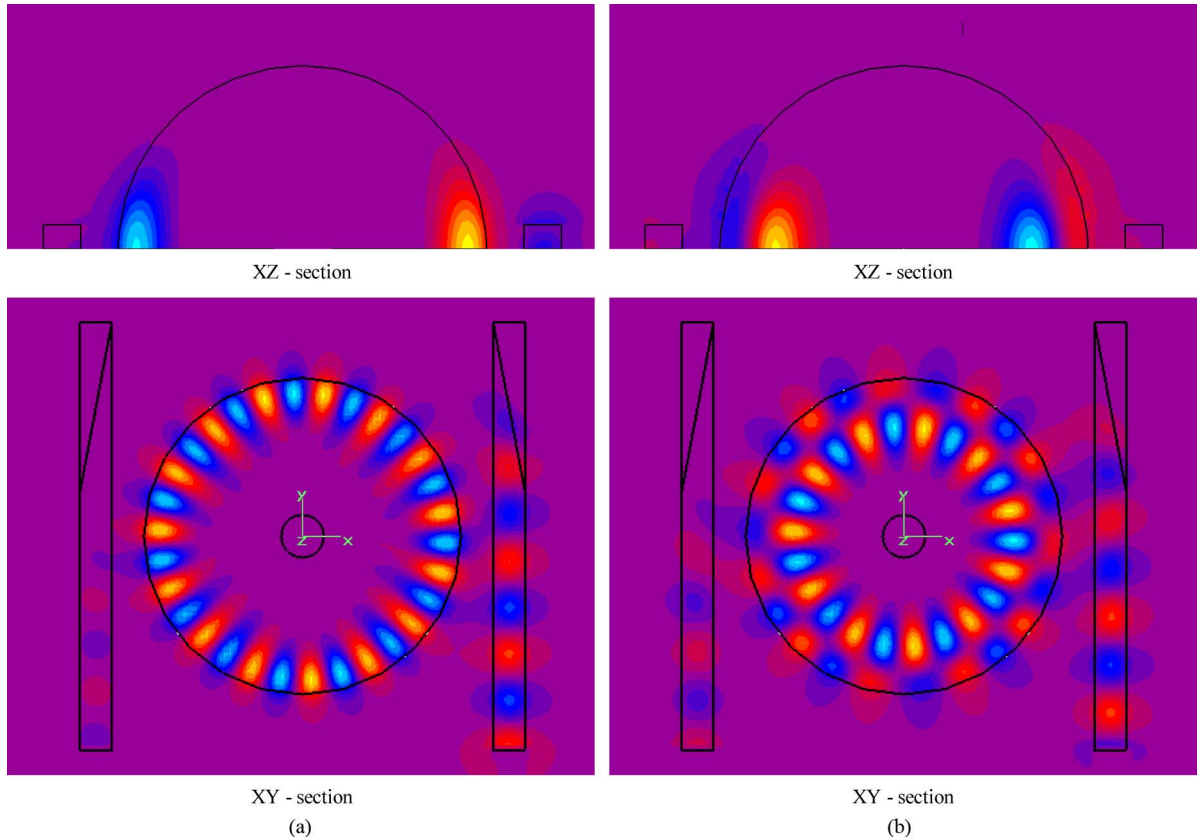


Fig. 4. Calculated distribution of field  $E_{zpv}$  component. (a)  $TE_{15\ 15\ 1}$  and (b)  $TE_{11\ 11\ 2}$  modes in a hemispherical whispering gallery mode resonator with conducting plane using MWS.

( $Al_2O_3$ ) resonator were measured. A permittivity tensor of a single-crystal sapphire can be expressed as the equation shown at the bottom of this page.

A hemisphere with radius  $r_1 = 0.741$  cm was produced with an optical axis perpendicular to the conducting copper plane of the resonator (see Fig. 1). The surface resistance of the copper plate was measured using a sapphire disc resonator and determined as  $55\ m\Omega$  at room temperature.

Since there is no analytic solution of the electrodynamic problem for an anisotropic hemisphere with a conducting plane, the sapphire resonator was numerically simulated using the MWS package (transient and eigenmode solvers). The resonance frequencies and field redistribution of the excited modes were calculated.

Fig. 4(a) and (b) shows the distributions  $E_{zpv} = -E_{\theta pv} \sin \theta$  of field components  $TE_{15\ 15\ 1}$  and  $TE_{11\ 11\ 2}$  modes, respectively, in the sapphire hemisphere whispering gallery mode resonator with a copper plate in the planes  $\varphi = 0$  (in  $XZ$  cross section) and  $\theta = \pi/2$  (in  $XY$  cross section). Excitation of the resonator was realized by a quasi-image sapphire waveguide ar-

ranged in a plane  $\theta = \pi/2$ . Fig. 4 demonstrates that the resonator fields of both modes are concentrated near the conducting plane. In the future, we will concentrate our studies on  $H$  modes in a hemisphere sapphire resonator, because for the  $H$  mode, the maximum density of the field energy spreads close to the metal plate surface [23], which indicates a preference of this mode for  $R_S$  measurements.

The frequency dependencies of the resonator  $S$ -parameters are shown in Fig. 5. The experimental data were measured in the frequency band from 30 to 40 GHz. In addition, the dependencies are calculated using MWS (Fig. 5). Both the calculated and measured frequency spectra are in good agreement. The relative difference of the calculated and measured frequencies does not exceed 1% and can be decreased easily by fitting the permittivity tensor.

The resonator modes are identified from a comparison of the calculated and measured mode frequencies and field structures. The slight deviation of the calculated and experimental results can be explained by a systematic inaccuracy of the numerical method defined in the program, which depends on the relation

$$\hat{\epsilon}_1 = \begin{pmatrix} 9.4(1 + 2.3 \times 10^{-5}i) & 0 & 0 \\ 0 & 9.4(1 + 2.3 \times 10^{-5}i) & 0 \\ 0 & 0 & 11.59(1 + 2.3 \times 10^{-5}i) \end{pmatrix}$$

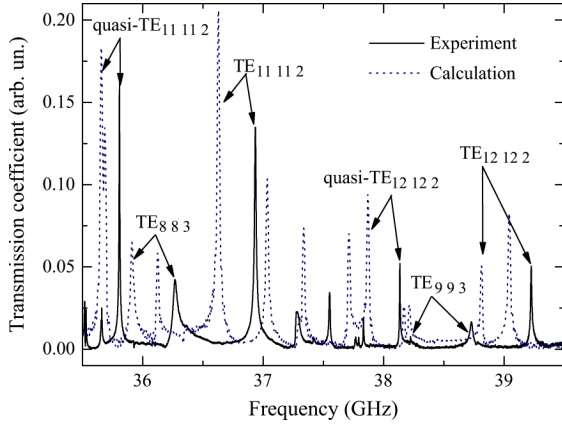


Fig. 5. Spectrum of the studied whispering gallery mode resonator designed from sapphire: dashed line—results of calculation (MWS), solid line—experimental results.

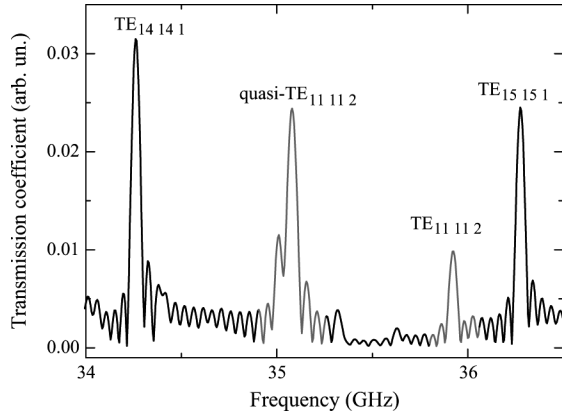


Fig. 6. Spectrum of whispering gallery mode hemispherical resonator designed from sapphire, calculated using MWS (for the case without a plate).

of the resonator wavelength and the dimension of the mesh cells of the studied structure. Additional resonance peaks are resolved in the calculated spectrum, and missing or weakly pronounced peaks in the measured spectrum.

The deviation can be explained by the difficulty in fulfilling the identity of excitation conditions for the resonator in these two cases.

It should be noted that the quasi- $TE_{n n 2}$  modes were excited in the studied resonator, containing all six components of electromagnetic fields, space distributions of which are identical to those of the corresponding  $TE_{n n 2}$  modes, except that the modes have only five field components because  $E_{r\nu\nu} \equiv 0$ . The quasi- $TE_{n n 2}$  modes are a result of anisotropy in the material of the spherical resonator made according to [25]. In addition, the quasi-TE modes are also registered in the hemispherical resonator without any conducting plane (Fig. 6). In the case of the isotropic material, the spherical resonator made from Teflon was only excited with the TE and TM modes, which have only five field components.

To study the anisotropy effect of a uniaxial single crystal on the properties of a whispering gallery mode resonator, the case of hemispherical resonators of  $r_1 = 0.741$  cm was calculated

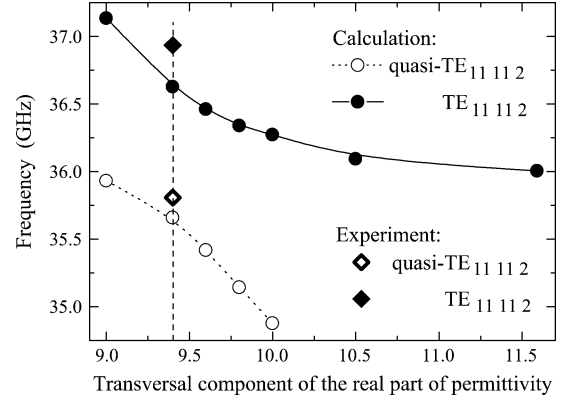


Fig. 7. Resonance frequencies of a hemispherical whispering gallery mode resonator with different kinds of anisotropy corresponding to the case of  $TE_{11 11 2}$  and quasi- $TE_{11 11 2}$  modes: closed symbols—TE modes, open symbols—quasi-TE modes.

numerically for dielectrics with different anisotropy. The dielectric permittivity was considered with a longitudinal (along the optical axis of crystal) component of  $\varepsilon_{1\parallel} = 11.59(1 + 2.3 \times 10^{-5}i)$  and with a transversal (in a perpendicular direction with respect to the optical axis of crystal) component of  $\varepsilon_{1\perp} = \varepsilon'_{1\perp}(1 + 2.3 \times 10^{-5}i)$ . The  $\varepsilon'_{1\perp}$  is varied in the interval from 4 to 11.59. In the resonators, the optical axis was perpendicular to the conducting plane. The calculation results of resonance frequencies for two modes are shown in Fig. 7. The indices of the resonator eigenmode was identified by analyzing field distribution in the resonator. This approach is used for experimental, as well as numerical (MWS) studies.

The results demonstrate that quasi- $TE_{11 11 2}$  and  $TE_{11 11 2}$  modes have only slightly different frequencies. This fact confirms that the nature of quasi-TE modes is related to the anisotropy of sapphire ( $\varepsilon'_{1\perp} = 9.4$ ). The resonance frequencies of  $TE_{n n 1}$  modes depend weakly on  $\varepsilon'_{1\perp}$  in comparison with quasi- $TE_{n n 2}$  ones.

For the application of a hemispherical sapphire resonator in microwave investigations of an HTS film surface  $R_S$  [21], [35], it is necessary to determine the conductor inclusion factor  $A_S^j$ . This factor cannot be calculated due to a lack of electrodynamic analysis for the case of an anisotropic resonator. Work on developing a technique for the determination of coefficient  $A_S^j$  in an anisotropic hemispherical resonator with a conducting plane and the method of  $R_S$  measurement is under way and will be published in a separate paper.

#### IV. CONCLUSION

The spectral and energy characteristics of a whispering gallery mode resonator in the form of a hemisphere with an impedance plane have been studied. An electrodynamic analysis of the resonator was carried out using Maxwell equations and an impedance boundary condition: the Leontovich boundary condition. It was shown that the inclusion factor  $A_S^j$  of a conductor in the resonator was determined by the field distribution and frequency of the  $j$ -type eigenmode in the resonator with a perfect conducting plane.

Results of the theoretical study and experimental measurements of the Teflon resonator frequency spectrum and  $Q$  factor agree well. The results were also confirmed by calculations using Microwave Studio CST 2008. It was found that the electromagnetic field localizes near the impedance plane.

In the case of a sapphire hemispherical resonator with an impedance plane, the results of the experiments are compared with a numerical simulation using Microwave Studio CST 2008 because, at the present, a characteristic equation and expressions for eigenmode field components in an anisotropic hemispherical resonator with an impedance plane cannot be calculated analytically. This approach allowed us to identify the  $H$ -type modes in the resonator by analyzing the distribution of the electromagnetic field. It was found that, in such a resonator, the quasi-TE modes are excited together with TE modes inherent to the isotropic resonator. It was established that the  $TE_{n n s}$  and quasi- $TE_{n n s}$  modes are excited with practically identical distribution of field components, which is confirmed by the coincidence of their mode indices. In the hemisphere sapphire resonator studied, the  $TE_{n n s}$  and quasi- $TE_{n n s}$  mode frequencies differ by approximately 1 GHz.

The results obtained show that high-quality hemisphere whispering gallery mode resonators can be applied in the microwave technique. In particular, they make it possible to improve the technique for measuring electrophysical parameters for different substances including HTS films. They can be used for the development of low-phase noise microwave oscillators including millimeter-wave oscillators and advanced dielectric resonator-based devices.

#### REFERENCES

- [1] S. J. Fiedziuszko and S. Holme, "Dielectric resonators," *IEEE Microw. Mag.*, vol. 2, no. 3, pp. 51–60, Mar. 2001.
- [2] V. S. Ilchenko and A. B. Matsko, "Optical resonators with whispering-gallery modes—Part II: Applications," *IEEE J. Sel. Topics Quantum Electron.*, vol. 12, no. 1, pp. 15–32, Jan.–Feb. 2006.
- [3] X. H. Jiao, P. Guillon, P. Auxtmery, and L. F. Bervudes, "Whispering-gallery modes of dielectric structures: Application to millimeter wave bandstop filters," *IEEE Trans. Microw. Theory Tech.*, vol. MTT-35, no. 11, pp. 1169–1175, Nov. 1987.
- [4] S. A. Vitusevich, K. Schieber, I. S. Ghosh, N. Klein, and M. Spinnler, "Design and characterization of an all-cryogenic low phase-noise sapphire  $K$ -band oscillator for satellite communication," *IEEE Trans. Microw. Theory Tech.*, vol. 51, no. 1, pp. 163–169, Jan. 2003.
- [5] E. N. Ivanov and M. E. Tobar, "Low phase noise microwave oscillators with interferometric signal processing," *IEEE Trans. Microw. Theory Tech.*, vol. 54, no. 8, pp. 3284–3294, Nov. 2006.
- [6] C. R. Locke, E. N. Ivanov, J. G. Hartnett, P. L. Stanwix, and M. E. Tobar, "Design techniques and noise properties of ultra-stable cryogenically-cooled sapphire-dielectric resonator oscillators," *Rev. Sci. Instrum.*, vol. 79, pp. 051301–1–12, 2008.
- [7] S. Kharkovsky, A. Kirichenko, and A. Kogut, "Solid-state oscillators with whispering-gallery-mode dielectric resonator," *Microw. Opt. Technol. Lett.*, vol. 12, no. 4, pp. 210–213, 1996.
- [8] J. Krupka, K. Derzakowski, A. Abramowicz, M. E. Tobar, and R. G. Geyer, "Use of whispering-gallery modes for complex permittivity determinations of ultra-low-loss dielectric materials," *IEEE Trans. Microw. Theory Tech.*, vol. 47, no. 6, pp. 752–758, Jun. 1999.
- [9] R. Ratheesh, M. T. Sebastian, P. Mohanan, M. E. Tobar, J. Hartnett, R. Woode, and D. G. Blair, "Microwave characterisation of  $BaCe_2Ti_5O_{15}$  and  $Ba_5Nb_4O_{15}$  ceramic dielectric resonators using whispering gallery mode method," *Mater. Lett.*, no. 45, pp. 279–285, 2000.
- [10] N. Cherpak, A. Barannik, Y. Prokopenko, Y. Filipov, and S. Vitusevich, "Accurate microwave technique of surface resistance measurement of large-area HTS films using sapphire quasi-optical resonator," *IEEE Trans. Appl. Supercond.*, vol. 13, no. 2, pp. 3570–3573, Jun. 2003.
- [11] N. T. Cherpak, A. A. Barannik, S. A. Bunyaev, Y. V. Prokopenko, and S. A. Vitusevich, "Measurements of millimeter-wave surface resistance and temperature dependence of reactance of thin HTS films using quasi-optical dielectric resonator," *IEEE Trans. Appl. Supercond.*, vol. 15, no. 2, pp. 2919–2922, Jun. 2005.
- [12] A. A. Barannik, S. A. Bunyaev, Y. V. Prokopenko, Y. F. Filipov, and N. T. Cherpak, "HTS surface impedance measurement device," U.S. Patent 16620, Feb. 2, 2006.
- [13] J. Krupka, J. Breeze, A. Centeno, N. Alford, T. Claussen, and L. Jensen, "Measurements of permittivity, dielectric loss tangent, and resistivity of float-zone silicon at microwave frequencies," *IEEE Trans. Microw. Theory Tech.*, vol. 54, no. 11, pp. 3995–4001, Nov. 2006.
- [14] J. Krupka, D. Mouneyrac, J. G. Hartnett, and M. E. Tobar, "Use of whispering-gallery modes and quasi-TE<sub>0</sub> np-modes for broadband characterization of bulk gallium arsenide and gallium phosphide samples," *IEEE Trans. Microw. Theory Tech.*, vol. 56, no. 5, pp. 1201–1206, May 2008.
- [15] M. Hein, *High-Temperature Superconductor Thin Films at Microwave Frequencies*, ser. Tracts in Mod. Phys. Berlin, Germany: Springer-Verlag, 1999, vol. 155.
- [16] S. N. Vlasov, "On "whispering gallery modes" in open resonators with dielectric rod," *Radiotek. Elektron.*, vol. 12, no. 3, pp. 572–573, 1967.
- [17] J. K. Wait, "Electromagnetic whispering gallery modes in a dielectric rod," *Radio Sci.*, vol. 2, no. 9, pp. 1005–1017, 1967.
- [18] M. Tobar and A. Mann, "Resonant frequencies of higher order modes in cylindrical anisotropic dielectric resonators," *IEEE Trans. Microw. Theory Tech.*, vol. 39, no. 12, pp. 2077–2083, Dec. 1991.
- [19] N. T. Cherpak, A. A. Barannik, Y. V. Prokopenko, and S. A. Vitusevich, "Microwave impedance characterization of large-area HTS films: Novel approach," *Supercond. Sci. Technol.*, vol. 17, pp. 899–903, 2004.
- [20] Z. Y. Shen, *High-Temperature Superconducting Microwave Circuits*. Boston, MA: Artech House, 1994.
- [21] N. T. Cherpak, A. A. Barannik, and S. A. Bunyaev, "Quasi-optical dielectric resonator-based technique of HTS film millimeter-wave surface resistance measurements: Three types of resonators," in *Proc. 38th Eur. Microw. Conf.*, Amsterdam, The Netherlands, Oct. 2008, pp. 807–811.
- [22] S. Kharkovsky, Y. Filipov, and Z. Eremenko, "Whispering gallery modes of an open hemispherical image dielectric resonator," *Microw. Opt. Technol. Lett.*, vol. 21, no. 4, pp. 252–257, 1999.
- [23] A. A. Barannik, S. A. Bunyaev, and N. T. Cherpak, "Hemispherical quasi-optical dielectric resonators as possible sensors for impedance measurement of superconductors," in *Proc. 5th Int. Phys. Eng. Millimeter and Sub-Millimeter Waves Symp.*, Kharkov, Ukraine, Jun. 2004, pp. 430–432.
- [24] A. A. Barannik, S. A. Bunyaev, N. T. Cherpak, and S. A. Vitusevich, "Quasi-optical dielectric resonators in the form of a truncated cone," *J. Lightw. Technol.*, vol. 26, no. 17, pp. 3118–3123, Sep. 2008.
- [25] Y. V. Prokopenko, T. A. Smirnova, and Y. F. Filipov, "Eigenmodes of an anisotropic dielectric ball," *Tech. Phys.*, vol. 49, no. 4, pp. 459–465, 2004.
- [26] J.-M. LeFloch, J. D. Anstie, M. E. Tobar, J. G. Hartnett, P.-Y. Bourgeois, and D. Cros, "Whispering modes in anisotropic and isotropic dielectric spherical resonators," *Phys. Lett. A*, vol. 359, no. 1, pp. 1–7, 2006.
- [27] Y. V. Prokopenko, Y. F. Filippov, I. A. Shipilova, and V. M. Yakovenko, "Whispering gallery modes in a hemispherical isotropic dielectric resonator with a perfectly conducting planar surface," *Tech. Phys.*, vol. 51, no. 2, pp. 248–257, 2006.
- [28] Y. V. Prokopenko and Y. F. Filippov, "Anisotropic disk dielectric resonator with conducting end faces," *Tech. Phys.*, vol. 47, no. 6, pp. 731–736, 2002.
- [29] A. M. Fatih, Y. Prokopenko, and S. Kharkovsky, "Resonance characteristics of whispering gallery modes in parallel-plates-type cylindrical dielectric resonators," *Microw. Opt. Technol. Lett.*, vol. 40, no. 2, pp. 96–101, 2004.
- [30] A. A. Barannik, Y. V. Prokopenko, Y. F. Filippov, N. T. Cherpak, and I. V. Korotash, " $Q$  factor of a millimeter-wave sapphire disk resonator with conductive end plates," *Tech. Phys.*, vol. 48, no. 5, pp. 621–625, 2003.
- [31] L. A. Vainstein, *Electromagnetic Waves*. Moscow, Russia: Sov. Radio, 1957.
- [32] L. D. Landau and E. M. Lifshitz, *Electrodynamics of Continuous Media*. New York: Cambridge Univ. Press, 1992.
- [33] T. Van Duzer and C. W. Turner, *Principles of Superconductive Devices and Circuits*. New York: Elsevier, 1981.

- [34] J. Krupka and J. Mazierska, "Single-crystal dielectric resonators for low-temperature electronics applications," *IEEE Trans. Microw. Theory Tech.*, vol. 48, no. 7, pp. 1270–1274, Jul. 2000.
- [35] A. A. Barannik, S. A. Bunyaev, and N. T. Cherpak, "On the low-temperature microwave response of a YBCO epitaxial film determined by a new measurement technique," *Low Temp. Phys.*, vol. 34, no. 12, pp. 977–981, 2008.



**Alexander A. Barannik** was born in Kharkov, Ukraine, on April 23, 1975. He received the Diploma degree in cryogenic technique and technology from the Kharkov State Polytechnic University, Kharkov, Ukraine, in 2000, and the Ph.D. degree (physical and mathematical sciences) in radiophysics from the Kharkov National University of Radio Electronics, Kharkov, Ukraine, in 2004.

Since 2000, he has been with the Institute of Radiophysics and Electronics, National Academy of Science of Ukraine, Kharkov, Ukraine, as a Junior Researcher (2000), Scientific Researcher (2005), and Senior Scientific Researcher (2007). He has coauthored over 50 scientific publications. He holds three patents. His scientific activities include the study of microwave characteristics of condensed matter, including HTS, dielectrics, and liquids by using whispering-gallery mode (WGM) dielectric resonators. He also studies electrodynamic properties of various types of WGM resonators.



**Sergey A. Bunyaev** (S'09) was born in Kharkov, Ukraine, on November 29, 1980. He received the B.S. and M.S. degrees in electronics from the Kharkov National University of Radio Electronics, Kharkov, Ukraine, in 2001 and 2002, respectively, and the Ph.D. degree (physical and mathematical sciences) in solid-state radiophysics from the Institute of Radiophysics and Electronics, National Academy of Science of Ukraine, Kharkov, Ukraine, in 2010.

From 2002 to 2009, he was with the Department of Solid State Radiophysics, Institute of Radiophysics and Electronics, National Academy of Science of Ukraine, Kharkov, Ukraine, as an Engineer (2002), doctoral student (2004), and Junior Researcher (2008). Since 2010, he has been with IFIMUP and IN-Institute of Nanoscience and Nanotechnology, Departamento de Física da Faculdade de Ciências, Universidade do Porto, Porto, Portugal. He has coauthored over 20 scientific publications. He holds two patents. His research interests include electromagnetics of microwave resonant structures, microwave high- $T_c$  superconductivity, and magnetic dynamics of patterned magnetic nanoelements and their arrays.



**Nickolay T. Cherpak** (M'01–SM'02) received the Ph.D. degree in radiophysics (including quantum radiophysics) from the Institute of Low Temperature Physics and Engineering, Kharkov, Ukraine, in 1970, and the Dr.Sc. degree in radiophysics from the Leningrad Polytechnic Institute (now Technical University), St. Petersburg, Russia, in 1987.

He is currently a Team Manager with the Department of Solid State Radiophysics, Institute for Radiophysics and Electronics, National Academy of Science of Ukraine, Kharkov, Ukraine, and a Professor with the Department of Technical Cryophysics, National Technical University-KhPI, Kharkov, Ukraine. In 1991, he was a Visiting Researcher with the University of Wuppertal, Wuppertal, Germany. In 2004, he was a Visiting Professor with the Institute of Physics, Chinese Academy of Sciences, Beijing, China. He has authored or coauthored about 280 papers in refereed journals and reports in scientific conferences. He authored *Millimeter-Wave Solid-State Maser Amplifiers of Distributed Type* (Naukova Dumka, 1996) and coauthored *Quasi-Optical Solid-State Resonators* (Naukova Dumka, 2009). He has also authored three scientific reviews. He holds 20 patents on various topics in microwave and millimeter-wave techniques. His current activity is in the area of development of techniques for millimeter-wave characterization of condensed matter, including

high-temperature superconductors and lossy liquids. He is also interested in the millimeter-wave physical study of condensed matter, especially high-temperature superconductors and electrodynamic properties of whispering-gallery mode (WGM) dielectric resonators.

Prof. Cherpak is a chairman of Commission E of the Ukrainian National URSI Committee. He was a program member of EuMW (2009 and 2010) and MMSW (1998, 2001, 2004, 2007, and 2010). He was the 1999 recipient of the I. Puljuy Award of Presidium of the National Academy of Sciences of Ukraine.



**Yurii V. Prokopenko** was born in the Kurgan Region, Russia, on October 20, 1961. He received the Diploma degree in radiophysics and electronics from the Kharkov State University, Kharkov, Ukraine, in 1987, the Ph.D. degree (physical and mathematical sciences) from the National Scientific Centre Kharkov Institute of Physics and Technology, Kharkov, Ukraine, in 1993, and the D.S. degree (physical and mathematical sciences) from the Usikov Institute of Radiophysics and Electronics, National Academy of Sciences of Ukraine, Kharkov,

Ukraine, in 2007.

From 1987 to 1994, he was a Researcher Fellow and from 1994 to 2000, he was a Senior Researcher with the National Scientific Centre Kharkov Institute of Physics and Technology. In 2000, he joined the Institute of Radiophysics and Electronics, National Academy of Sciences of Ukraine. He was involved with theoretical and experimental investigations of microwave oscillations and antennas, theoretical and experimental radiophysics, physics of charge particles, and the accelerator technique. He has authored or coauthored over 120 publications, and one monograph. He holds six invention certificates. He coauthored a high-power pulse microwave generator of a vircator type with a controlled feedback that was called the virtod. His current research activity includes theoretical electrodynamic properties of dielectric (and also semiconductor and ferrite) cylindrical, sphere, and hemisphere resonators.



**Anna A. Kharchenko** (S'08) was born in Kharkov, Ukraine, on February 22, 1986. She received the B.S. and M.S. degrees in mathematics and computer science from the Kharkov National University of Radioelectronics, Kharkov, Ukraine, in 2007 and 2008, respectively, and is currently working toward the Ph.D. degree at the Usikov Institute of Radiophysics and Electronics, National Academy of Sciences of Ukraine, Kharkov, Ukraine.

She has coauthored over ten scientific publications. Her main research interests are experimental microwave radiospectroscopy of periodical structure (metamaterials), investigation of Tamm-states, left-handed media (LHM) properties, metamaterial applications, and quasi-optical resonators.



**Svetlana A. Vitusevich** received the M.Sc. degree in radiophysics and electronics from Kiev State University, Kiev, Ukraine, in 1981, and the Ph.D. degree in physics and mathematics and Dr.habil degree from the Institute of Semiconductor Physics (ISP), Kiev, Ukraine, in 1991 and 2006, respectively.

From 1981 to 1997, she was with the ISP as Researcher (1981), Scientific Researcher (1992), and Senior Scientific Researcher (1994). From 1997 to 1999, she was an Alexander von Humboldt Research Fellow with the Institute of Bio- and Nanosystems (IBN) (formerly the Institute of Thin Films and Interface), Forschungszentrum Jülich (FZJ), Jülich, Germany. Since 1999, she has been a Senior Scientific Researcher with the FZJ. She has authored or coauthored 110 papers in refereed scientific journals. She holds eight patents, among which two of them are for semiconductor functional transformers. Her research interests include transport and noise properties of different types of materials for advanced electronic devices and circuits.